LA-UR-01-4983

Recent Results of Radiation Hydrodynamics and Turbulence Experiments in Cylindrical Geometry

G. R. Magelssen, S. H. Batha, C. W. Barnes, N. E. Lanier, R. D. Day, J. M. Scott, N. E. Elliot, R. L. Holmes, D. L. Tubbs*1*, A. M. Dunne, S. Rothman, D. L. Youngs*2*

1Los Alamos National Laboratory, Los Alamos, NM, 87545
2AWE Aldermaston, United Kingdom

Cylindrical implosion experiments at the University of Rochester laser facility, OMEGA, were performed to study radiation hydrodynamics and compressible turbulence in convergent geometry. Laser beams were used to directly drive a cylinder with either a gold (AU) or dichloropolystyrene (C*6*H*8*CL*2*) marker layer placed between a solid CH ablator and a foam cushion. When the cylinder is imploded the Richtmyer-Meshkov instability and convergence cause the marker layer to increase in thickness. Marker thickness measurements were made by x-ray backlighting along the cylinder axis. Experimental results of the effect of surface roughness will be presented. Computational results with an AMR code are in good agreement with the experimental results from targets with the roughest surface. Computational results suggest that marker layer "end effects" and bowing increase the effective thickness of the marker layer at lower levels of roughness.

Introduction

Mix experiments were performed on the OMEGA laser [1] at the Laboratory for Laser Energetics of the University of Rochester. In this paper experimental results from these experiments are compared to simulations. Laser beams were used to drive directly a cylindrical target with a marker layer placed between an ablator and a foam cushion[2-4]. As the cylinder implodes the marker layer thickness increases as a result of convergence and instabilities. This increased thickness is the indicator of the amount of mix occurring. To measure the thickness, the imploding cylinder is radiographed with x rays from a laser-heated titanium or iron foil normal to the cylinder along its axis. Use of the cylindrical geometry allows convergent interfaces to be observed directly from the side.

The entire cylinder implodes in an hourglass shape from the variation in intensity along the axial direction and from the large pressure differences at the ends of the cylinder. The ablator thickness was chosen to minimize the amount of acceleration after the initial shock passage through the marker. The shock generates a Richtmyer-Meshkov instability with compressible effects. At very late times the foam creates enough backpressure to decelerate the marker layer causing a very weak Rayleigh-Taylor instability. Thus, the turbulence is primarily driven by the passage of a single shock across a perturbed, variable density interface.

Experiment

The experiment was designed to create a uniform illumination region in the central region of the cylinder where the 500 μm marker layer was located. For the target, a marker layer of either gold or dichloropolystyrene ($C_6H_8CL_2$) was placed between polystyrene (solid CH) and a polystyrene foam (60 mg/cm^3). The marker material is chosen to be more opaque to the backlighter x rays and to have a different density from the ablator or foam. The polystyrene cylinders were 2.25-mm long with 0.86-mm inner diameter. They were illuminated with 351-nm wavelength light from 50 laser beams in a 1-ns square laser pulse. The total laser energy was 19 to 20 kJ with less than 8% RMS variation in energy balance.

Two different types of gold marker layer surfaces were developed: rough and smooth. The rough Au was made by vapor depositing Au onto foam cylinder. The gold was observed by SEM to lie conformally on the rough foam surface, and its thickness determined to be 0.85 ± 5 μm from two different techniques, x-ray radiography and x-ray fluorescence. The smooth gold was measured by fluorescence to be 1.0 ± 0.05 μm. Figure 1 illustrates the measurements of the surfaces for gold and shows how the power per unit wavenumber of the surface roughness decreases with wavenumber k as k-*3/2* for the gold-on-foam. The machined styrene decreased as k-*2*. Notice that the smooth gold is three orders of magnitude less rough than the gold-on-foam.

Two different sets of experiments will be presented. For the first, experiments with marker layers at opposite extremes are compared. A “low-mix” system with a “smooth” 4

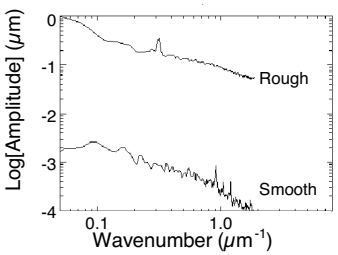

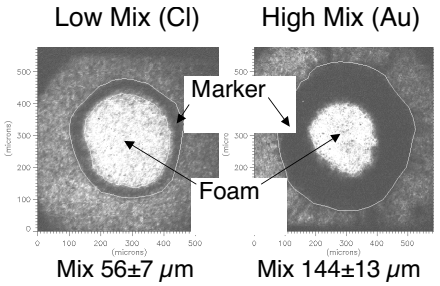

Fig. 1. Surface roughness spectra for

μm thick dichloropolystyrene marker is compared to a "high-mix" system with 0.85 μm of rough gold. The ablators were made thick, consisting of 73 μm polystyrene over the low-mix dichloropolystyrene marker or 60 μm polystyrene over the high-mix gold. This design choice matches the total mass between the systems, with the pusher thickness determined so that the shock breaks out from the pusher at the end of the laser pulse. The extent of the mixing of the materials across the interfaces is what is measured. Figure 2 shows typical axial radiographs for both low-mix and high-mix cases. The chlorinated marker was radiographed with 4.7-keV titanium k-shell x rays whereas 6.9-keV iron was used for gold. The frames are chosen to be at the same time (4.75 ± 0.10 ns) during the respective implosions, which had incident laser energy within 1.4% of each other. The fundamental result is that we see a relatively thin marker layer with the low-mix, initially smooth, chlorinated system but a very thick mix region with the high-mix, initially rough, gold system.

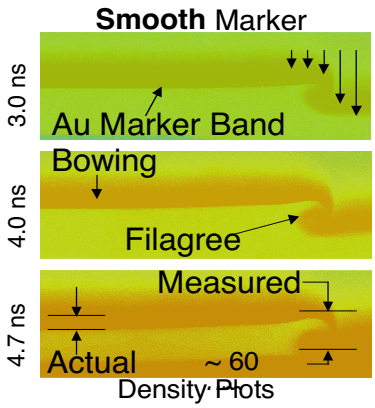

Fig. 4 Rage simulation of the smooth gold Marker layer

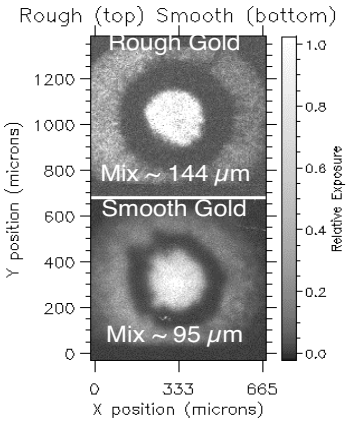

Fig. 3 Experimental radiographs of smooth and rough Gold marker bands

For the second set of experiments the rough and smooth gold marker layers are compared. The ablator was 60 ± 1 micron. The radiographic images were again taken at 4.75 ± 0.10 nsec and are given in Fig. 3. This experiment illustrates that increasing the marker layer roughness increases the mix width. However, the smooth result has a much larger width than expected from 1-D simulations suggesting other physical effects in addition to mix. The 4.7-keV titanium or 6.9-keV iron K-shell x rays are not energetic enough to transmit through the mixed gold, and only a mix width and not a radial density distribution can be determined from the present experiment.

Simulations

Many different hydrocodes are being used to try to predict our experimental results. Here we present only the Los Alamos effort. The group at AWE has done similar simulations with their code PETRA and a three-dimensional code called TURMOIL [5]. Direct comparisons of the calculated mix evolution with experiment use the 2D Lagrangian hydrocode LASNEX [6] to calculate the axial implosion profile along the radial direction r and axial direction Z assuming symmetry in the azimuthal direction. The AMR code RAGE [7,8] is used to compare with LASNEX and to calculate the turbulent mixing in the r-Z or r-Θ _planes, assuming symmetry in the azimuthal or axial directions, respectively.

LASNEX calculations were done totally integrated using the measured laser power profile and the three-dimensional laser raytrace package. However, including the surface roughness in the calculation was not possible with LASNEX. The calculations were done LTE (Local Thermodynamic Equilibrium) with thermal conduction and multigroup diffusion radiation transport. Thus, the LASNEX calculations give the expected "zeroth-order" hydrodynamics including any bowing of the marker and including effects at the ends of the marker.

The RAGE simulations were performed without laser deposition (not available), a two-temperature one group (grey) radiation diffusion model (muligroup not available) and thermal conduction. For RAGE the energy was sourced into 4 to 5 microns of the outer layer of the ablator. The energy was sourced uniformly over time and space for a 1 nsec period. For RAGE, both smooth and surface roughness calculations were done and the material interface roughness spectra were used. The calculations confirm that the laser-driven shock (about mach 5) reaches the interface at the end of the laser pulse, leading to a minimal period of interface acceleration during the laser drive and thus minimizing Rayleigh-Taylor growth in the early stages.

LASNEX radiographic images of the chlorinated marker thickness were about 15 μm what one would expect in a one-dimensional calculation. The gold thickness on the other hand is 45 microns, ten times the thickness of a one-dimensional simulation. The RAGE simulations clearly illustrate this large growth. Figure 4 shows three snapshots of a smooth surface gold simulation. The plot shows the gold bowing in the middle and vortex structures at the ends of the marker. Because gold is so opaque to 6.9 keV x rays the bowing and ends greatly increase the measured thickness of the calculated radiographic image. The calculated RAGE image is given in Fig. 5. As the cylinder implodes the less massive ablator (CH)

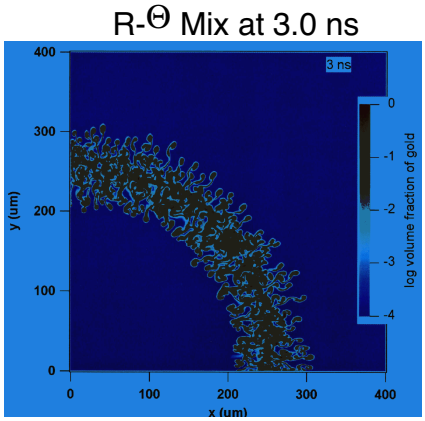

accelerates to a higher velocity than the gold. As it moves past the gold ends, velocity shear causes some of the gold to follow creating a complex velocity (vortex) and pressure pattern. The extent of the structure increases with time. By 4.7 nsec the simulation predicts a thickness of 50 to 60 microns a little larger than predicted by LASNEX and less than the 95 microns seen experimentally. A similar vortex structure occurs for the chlorinated marker. Although this marker's opacity is much less than gold, the lower backlighter energy caused the end structure to be opaque. The RAGE simulation gave a radiographically calculated thickness of 30 microns, larger than LASNEX and less than the measured value of 56 microns. The final RAGE simulation used the measured rough surface gold spectra. The r-Θ volume fraction profile at 3 nsec is shown in Fig. 6 indicating a marker width of 100 μm. The calculated and experimental comparison for this case is given in Fig. 7. The pictured linear increase in thickness as a function of time is consistent with RM growth.

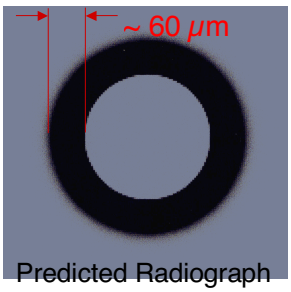

Fig. 5 Rage simulation of the smooth gold radiographic image showing a much enhanced marker thickness

Conclusions

In conclusion, this experiment demonstrates the ability to perform quantitative measurements of mix in convergent geometry using compressible plasmas. It provides a well-posed test of an integrated modeling capability and acts as the basis for generating 1D mix 'models' [9] which capture the essential growth characteristics. Because of space constraints we can't list all the relevant references related to this work. A few are listed [10-13]. We acknowledge the vital technical contributions of Pete Walsh, Scott Evans, Tom Ortiz, Tom Sedillo, John Oertel, Ken Klare, Harry Bush, Joyce Elliott, Doug Hatch, Kett Gifford, Pete Gobby, Veronica Gomez, Ruben Manzanares, Tim Pierce, Lee Salzar, David Sandoval, Corky Thorn, and Colin Horsfield. We also thank John Soures, Sam Morse, Greg Pien, Christian Stoeckl, Keith Thorp, and the rest of the OMEGA operations staff.

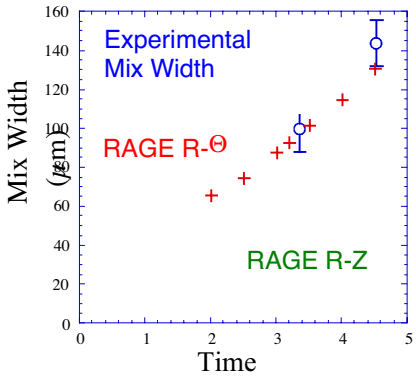

Fig. 7 Experimental results and simula are consistent with linear growth sugge that RM is the dominant instability

References

[1] T. R. Boehly, *et al*., Optics Communications **133**, 495 (1997).
[2] D. L. Tubbs, *et al*., Laser Part.Beams **17,** 437 (1999).
[3] D. L. Tubbs, *et al*., Phys. Plasmas **6,** 2095 (1999).
[4] C. W. Barnes, *et al*., Rev. Sci. Instrum. **70,** 471 (1999).
[5] A. M. Dunne, *et al*., 'personal communication'
[6] G. B. Zimmerman and W. L. Kruer, Comments Plas. Phys.**2,** 51 (1975).
[7] M. L. Gittings, Defense Nuclear Agency Numerical Methods Symposium, 28-30 April 1992.
[8] R. L. Holmes, *et al*., J. Fluid Mech. **389,** 55 (1999).
[9] D. L. Youngs, Laser Part. Beams **12,** 725 (1994).
[10] M. B. Schneider, *et al*., Phys. Rev. Lett. **80,** 3507 (1998).
[11] S. T. Weir, *et al*., Phys. Rev. Lett. **80,** 3763 (1998).
[12] T. A. Peyser, *et al*., Phys. Rev. Lett. **75,** 2332 (1995).
[13] G. Jourdan, *et al*., Phys. Rev. Lett. **78,** 452 (1997).